Electronic Supplementary Material (ESI) for Lab on a Chip.

Supplemental Information

Performing multi-step chemical reactions in microliter-sized droplets by leveraging a simple passive transport mechanism

Jia Wang[1,2], Philip H. Chao[1,2], Sebastian Hanet[1], R. Michael van Dam[1,2,*]

[1] Crump Institute for Molecular Imaging and Department of Molecular & Medical Pharmacology, David Geffen School of Medicine, University of California at Los Angeles (UCLA), Los Angeles, CA, USA

[2] Department of Bioengineering, ULCA, Los Angeles, CA, USA

* Corresponding author: mvandam@mednet.ucla.edu

Table of Contents

1 Microfluidic chip fabrication

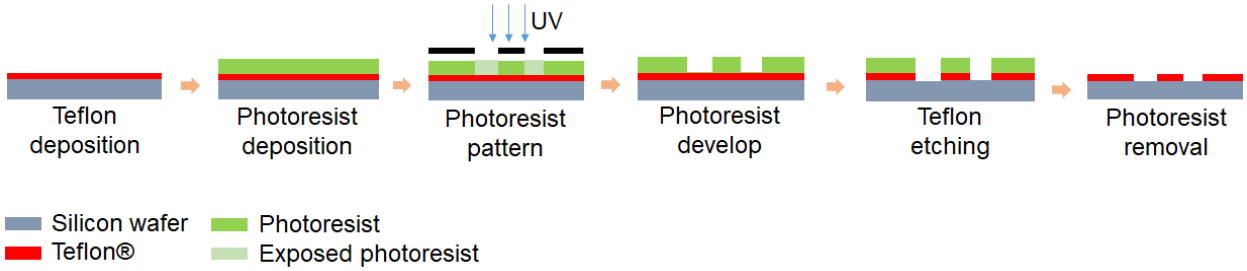

Figure S1. Schematic of microfluidic chip fabrication process. A silicon wafer is first spin-coated with Teflon® AF 2400. The Teflon is patterned by first spin-coating and patterning photoresist as an etch mask, and then removing exposed Teflon via dry-etching. Finally the water is diced into individual chips and each chip is subject to photoresist removal and treatment with Piranha solution to increase hydrophilicity of patterned pathways.

Treatment	Contact angle (°) (n=3)
Initial Si wafer	41 ± 4
Hydrophobic region before patterning	122 ± 2
Hydrophilic region (after acetone wash)	57 ± 10
Hydrophilic region (after Piranha clean)	7 ± 3

Table S1. Contact angle measurements of a droplet of DI water (~2 µL) on the microfluidic chip at different stages during the fabrication process.

2 Characterization of droplet transport rate

A simple chip design, consisting of a single delivery channel connected to a circular reaction zone, was fabricated to evaluate suitability of passive transport for various aqueous and organic solvents (**Figure S2A**). Taper angles α were varied in 1° increments from 1° to 10° to investigate the droplet movement behavior. Video of droplet movement on the chip was recorded with an iPhone 7 camera at 60 fps (1080p HD). Transporting time was calculated by subtracting starting frame number (droplet just loaded on the pathway, **Figure S2B**) from ending frame number (droplet just reached the reaction zone, **Figure S2C**).

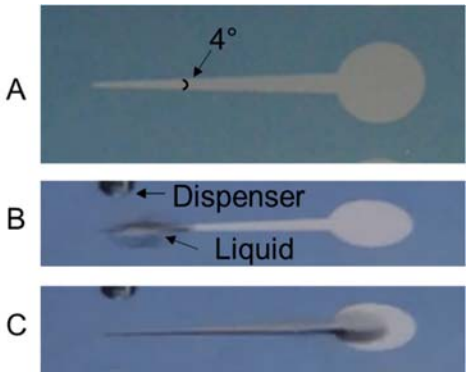

Figure S2. (A) Photograph of the simple passive microfluidic chip for characterizing droplet movement (top view). The taper angle of the pathway in this particular chip was 4°. (B) Video frame from video recording of 1 µL DI water on the pathway. Note that for practical reasons, the video was taken at a slightly oblique angle above the chip. The frame shows the droplet has just been deposited at the start of the pathway and was defined as starting frame. (C) Video frame showing the same droplet at the time it reached the reaction site (defined as the ending frame). The number of intervening frames could be used to compute the transport time.

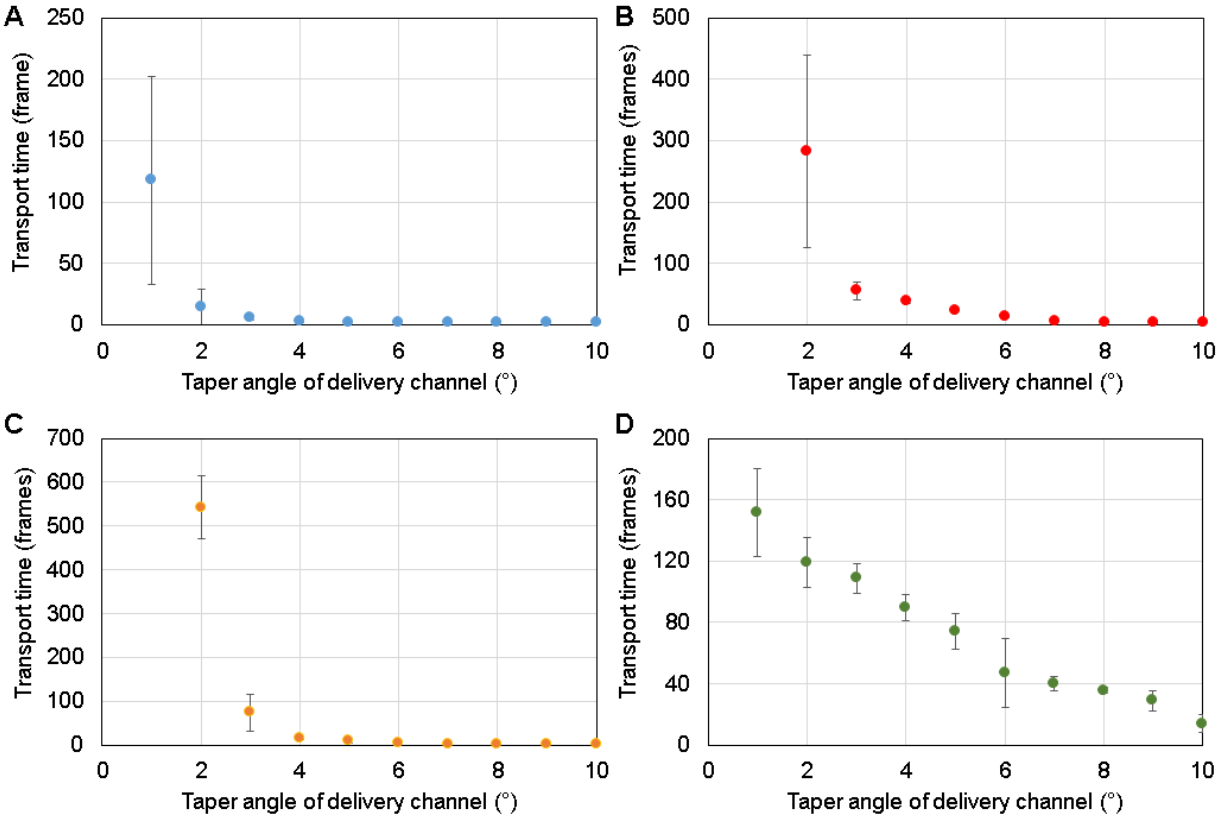

Figure S3. Moving rate of different solvents as a function of taper angle of the reagent delivery pathway. (A) 1 µL droplet of DI water (n=4). (B) 1 µL droplet of MeOH (n=4). (C) 1 µL droplet of MeCN (n=4 for 1-5°; n=2 for 6-10°). (D) 1 µL droplet of DMSO (n=3). Note that if the time to reach the reaction site exceeded 1000 frames, the transport speed was considered to be zero and the data was omitted from the graph (i.e. 1° taper angle for MeOH and MeCN). All solvents were deposited via non-contact dispensers (INKX0514300A for DI water, MeOH and MeCN; INKX0514100A for DMSO).

3 Characterization of dispensing volumes

Dispense volumes by the non-contact dispensers were measured by averaging the weight of dispensed solutions. The dispenser was opened for a certain duration at 5 psi and the dispensed solution was collected in an empty PCR tube. After n=10 such droplets were dispensed, the total mass of the dispensed liquid was determined on an analytical balance. Using the known density of the solution at room temperature, the total volume was determined. The average volume of an individual droplet was determined by dividing by n=10. Plots of dispensed volume versus valve opening time are shown in **Figure S4**. The relationship was approximately linear for times > 10 ms. The curves could be used to determine the necessary time to dispense a particular volume.

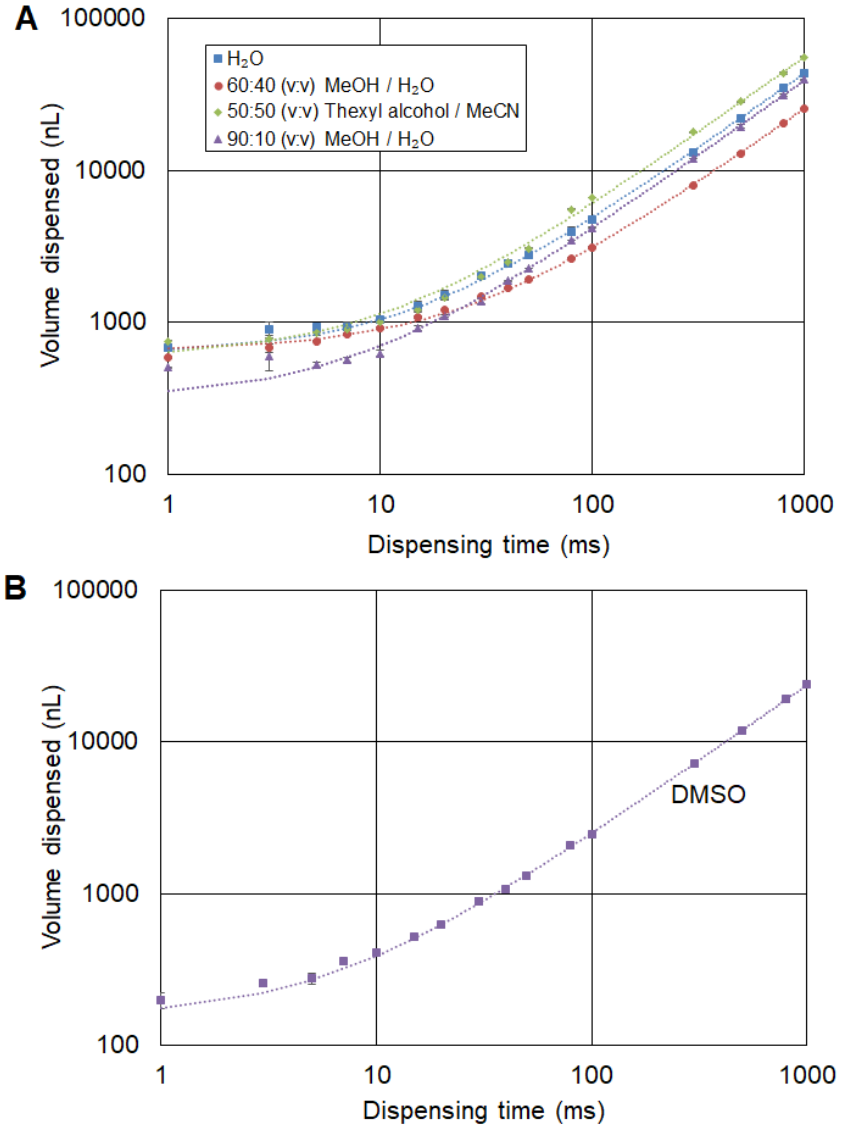

Figure S4. Calibration curves for dispensed droplet volume. (A) Various solvent mixtures using INKX0514300A dispensers with solvent reservoir pressurized to 5 psi. Trend lines are linear fits with R^2 values of 0.9999 for DI water (H_2O), 0.9999 for 60:40 v/v MeOH / H_2O, 0.9995 for 50:50 v/v thexyl alcohol / MeCN, and 0.9998 for 90:10 v/v MeOH / H_2O. (B) DMSO dispensed with INKX0514100A dispenser and reservoir pressurized to 7 psi. R^2 for the linear fit was 1.0000.

4 Characterization of capacity of reaction site

Passive transport chips of six pathways and one reaction site were fabricated as described in the main paper. Droplets of various sizes (0.5 μL, 1 μL, 1.5 μL, 2 μL, 5 μL) were manually loaded on the narrow end of bottom pathway (**Figure S5**). Photos were taken at the moment when solvents stopped moving. For DI water, the majority of the droplet maintained in the reaction site for droplet volumes smaller than 2 μL. MeOH and MeCN behaved similarly to DI water. The higher evaporation rate may help to prevent overflow of the reaction site. DMSO easily overflowed even with the lowest (0.5 μL) droplet volume.

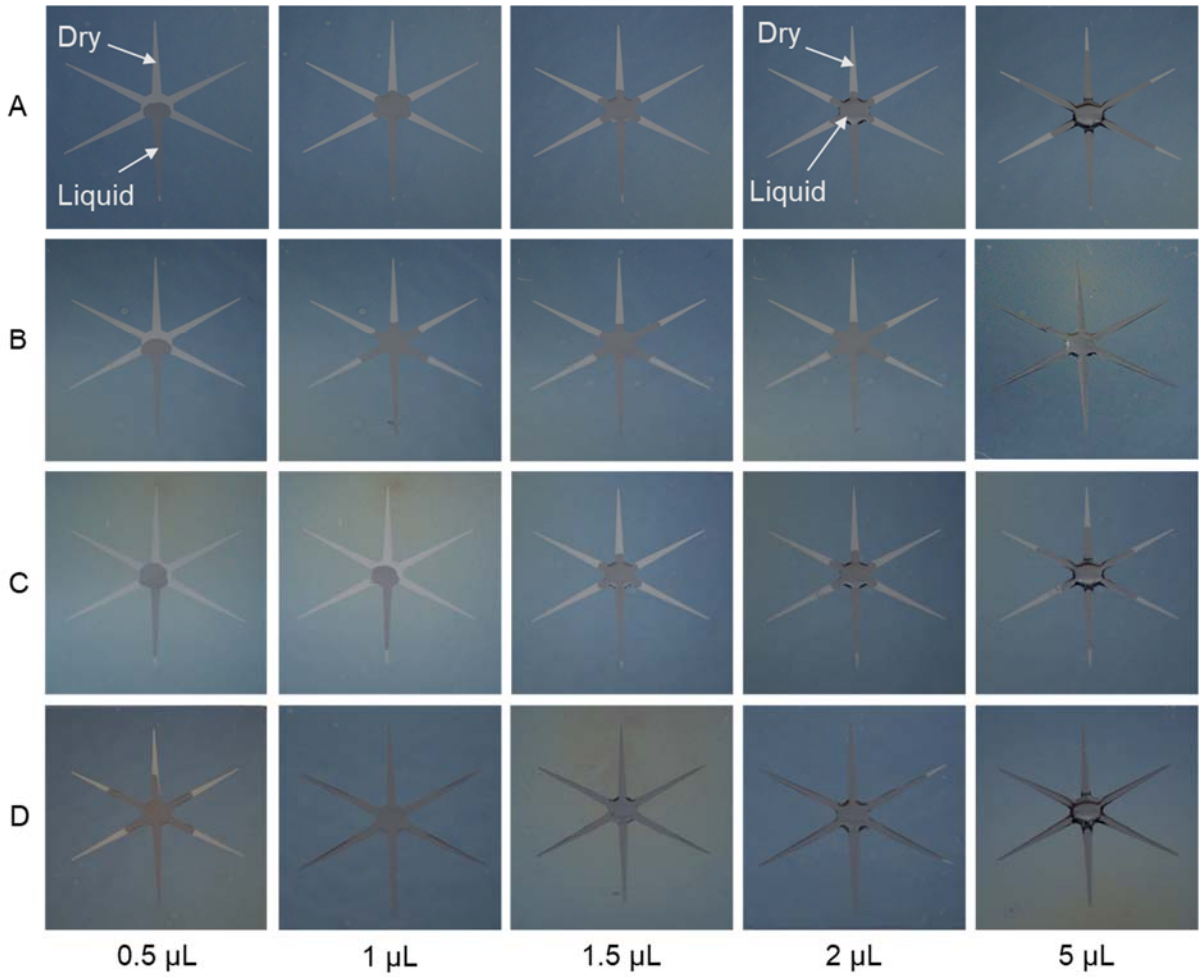

Figure S5. Behavior of solvents droplets of different volumes after reaching the reaction site. (A) DI water; (B) MeOH; (C) MeCN; (D) DMSO.

5 Optimization of protocol for [^{18}F]FDG synthesis using Cerenkov imaging

To find conditions that avoided overflowing of the reaction site when loading 2 µL of this radioisotope solution, different loading methods were explored. [^{18}F]fluoride/[^{18}O]H_2O was premixed with $K_{2.2.2}$ (133 mM)/K_2CO_3 (33 mM). This solution was then loaded and dried by various methods. Cerenkov images were taken and processed as described in the main paper.

When a single 2 µL droplet was loaded on the pathway and dried at 105°C for 1 min, we observed significant spreading of the solution along reagent pathways during evaporation, leading to significant radioactive residue outside the reaction site (**Figure S6A**). For smaller droplets (0.5 µL, 1 µL), heating was applied to the chip after first droplet was loaded, and subsequent droplets were loaded sequentially while the chip was heated until a total of 2 µL had been loaded. For the 1 µL droplets, the Cerenkov image after completion of this step showed that the radioactivity remained confined within the reaction site (**Figure S6B**). For the 0.5 µL droplets, the first droplet exhibited spreading along the reagent pathways, and the following droplets dried on the pathway before getting to the reaction site because of rapid evaporation (**Figure S6C**). Due to the reliable confinement of radioactivity using two 1 µL droplets, subsequent experiments were performed in this manner.

Next, the concentrations were varied to optimize the yield. Optimal results were obtained when the [^{18}F]fluoride/[^{18}O]H_2O was premixed with K222 (40 mM)/K_2CO_3 (22 mM). Cerenkov imaging revealed that the residue remained confined to the reaction site with this new composition (**Figure S6D**).

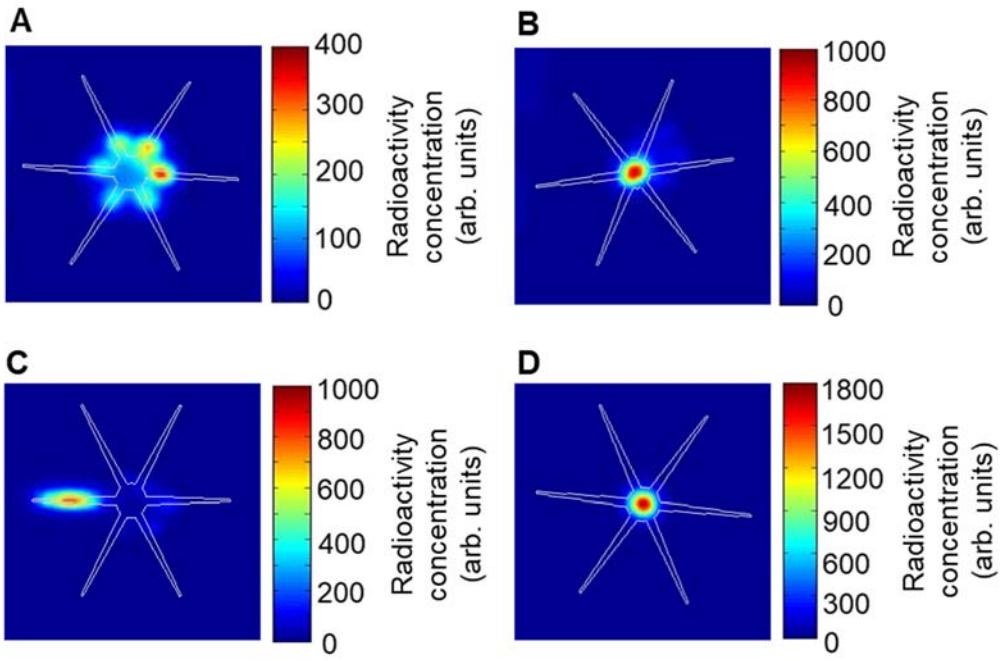

Figure S6. Distribution of radioactivity after [^{18}F]fluoride drying step of [^{18}F]FDG synthesis visualized using Cerenkov imaging. (A) A single 2 µL droplet of [^{18}F]fluoride solution (with 133 mM $K_{2.2.2}$ and 33 mM K_2CO_3) was loaded and dried; (B) Two 1 µL droplets were loaded and dried sequentially; (C) Four 0.5 µL droplets were loaded and dried sequentially; (D) A single 2 µL droplet of [^{18}F]fluoride solution (with 40 mM K222 and 22 mM K_2CO_3) was loaded and dried.